Building a super-resolution fluorescence cryomicroscope

Mart G. F. Last[1], Lenard M. Voortman[1], Thomas. H. Sharp[1]*

[1]Department of Cell and Chemical Biology, Leiden University Medical Centre, 2300 RC Leiden, The Netherlands

*To whom correspondence should be addressed: t.sharp@lumc.nl

Abstract

Correlated super-resolution fluorescence microscopy and cryo-electron microscopy enables imaging with both high labelling specificity and high resolution. Naturally, combining two sophisticated imaging techniques within one workflow also introduces new requirements on hardware, such as the need for a super-resolution fluorescence capable microscope that can be used to image cryogenic samples. In this chapter, we describe the design and use of the 'cryoscope'; a microscope designed for single-molecule localization microscopy (SMLM) of cryoEM samples that fits right into established cryoEM workflows. We demonstrate the results that can be achieved with our microscope by imaging fluroescently labelled vimentin, an intermediate filament, within U2OS cells grown on EM grids, and we provide detailed 3d models that encompass the entire design of the microscope.

Introduction

Correlating super-resolution fluorescence microscopy and cryo-transmission electron microscopy (cryoEM) opens up new avenues for studying biological systems at high-resolution and in native conditions[1–3]. Super-resolution fluorescence provides highly precise contrast by labeling specific components, but lacks informative content for anything other than the labelled structure. Conversely, cryoEM offers high-resolution imaging of cells in their native state, but with less specificity: contrast is based on the electron density of the entire, unlabelled, sample.

To combine these two techniques, a fluorescence microscope is required that achieves a high enough resolution for accurate correlation with cryoEM, and with which cryosamples can be imaged. In this chapter, we demonstrate a blueprint for a single molecule localization cryomicroscope (cryoSMLM), and we outline the steps involved in constructing and operating this 'cryoscope'. We also provide some representative data where we have used our cryoscope to perform correlative super-resolution cryo-fluorescence microscopy and cryo-electron microscopy (SR-cryoCLEM).

At a cost of only between 1-2% that of a high-end cryoEM, and less than commercial widefield or confocal cryo-microscopes, the cryoscope can be used to locate sites of interest for cryoEM inspection with high spatial accuracy, to enrich cryoEM data by providing additional cellular context via fluorescent labelling, to screen sample thickness[4] without requiring access to a TEM, and for numerous other applications. In our lab, the cryoscope is a cornerstone of our high-resolution cellular imaging workflow: it is routinely

used for the acquisition of single molecule localization maps with ~30 nm resolution, which are instrumental in targeting the acquisition of and identification of biomolecules within cryo-electron tomography datasets.

Overview

While there are numerous super-resolution imaging methods available that would be suited for correlation with cryoEM imaging[5–8], the microscope described here is specifically designed for single molecule localization microscopy (SMLM)[9], a subset of super-resolution imaging techniques comprising methods such as photo-activated localization microscopy (PALM)[10] and stochastic optical reconstruction microscopy (STORM)[11].

Many designs have been published for conventional ambient-temperature SMLM microscopes[12], and the novel requirement of maintaining samples in cryogenic conditions indeed does not change every aspect of an SMLM microscope; e.g., the image forming part of the optical system is agnostic of sample conditions. Because of the significant overlap between room-temperature SMLM microscopes and the design described here, we focus only on those features of the design and operation that are specific to cryo-microscopy, and refer the reader to previously published work for other 'standard' aspects[13,14].

[FIGURE 1 GOES HERE]

Cryo-specific design considerations

Laser light source

SMLM methods rely on stochastic or controlled blinking of fluorescent molecules. Typically, high illumination power densities are required to achieve control over the emissive state of certain fluorescent dyes and proteins[15,16], such as the reversibly photo-switchable green fluorescent protein rsEGFP2 (Figure 1), which is activated (converted to a fluorescent 'on' state) with 405 nm light and excited and de-activated (converted to a dark 'off' state) with 488 nm illumination. While the switching mechanisms of photo-switching fluorescent proteins are not entirely understood, particularly in cryogenic conditions[3], it is known that photo-switching rates are significantly reduced at low temperatures[15,17]. Thus, to perform SMLM with fluorescent proteins in cryogenic conditions, multiple high power light sources are required, which are invariably laser light sources.

Samples

High illumination power densities pose somewhat of a problem in cryogenic conditions, as the heat generated by absorption of light can lead to destruction of the sample. This issue has prompted the investigation of alternative super-resolution methods for imaging cryosamples[6,18], and might in the future be avoided by the development of novel fluorescent probes that require less intense illumination to blink[19]. Currently, the way to avoid light-induced damage while using high illumination power densities is to select specific support grids that are capable of withstanding high illumination power densities,

such as grids with low absorption support film, high mesh numbers, or grids with a low fraction of the area covered by absorbing material[20,21].

LED light source

Next to the laser light source for fluorescence activation and excitation, the microscope is equipped with a multi-color LED light source for epi-illumination. This source is not required for super-resolution fluorescence imaging, but it enables an accurate and rapid measurement of the sample thickness using a method that we have recently developed[4] (Figure 1, panel 2). The ability to assess sample thickness in the light microscope is hugely beneficial in a correlated experiment, as it helps to determine whether a site is suited for cryoEM prior to actually taking the sample to the cryoEM. Moreover, by simply locating naturally thin regions of interest, the costly and time-consuming use of cryo-focused ion beam (FIB) milling can also be avoided.

While a multi-color LED light source is required for thickness inspection, reflected light images acquired with any single LED source can be useful in correlating light to electron microscopy images. For most grid types, reflection contrast is mainly based on the reflectivity of the sample supporting film. In TEM images, the support film is also easily recognized. Reflection images can therefore be used as a 'bridge' between fluorescence and TEM images: a reflected light image contains features that are visible in the TEM, and is registered in the same coordinate system as fluorescence images.

Objective lens

With few exceptions, fluorescence cryo-microscopy is performed using dry lenses, i.e., without the use of immersion media. While immersion lenses can offer a higher numerical aperture (NA), technical challenges in maintaining a temperature gradient between the sample and the warmer objective lens as well as the requirement for media that remain liquid at ~76 K render the use of immersion lenses rather impractical. It is worth noting however that cryo-microscopes using liquid and solid immersion objective lenses have been described[22,23]. Regardless, with an NA of 0.9, we routinely achieve a localization precision of 30 nm.

Besides the NA, the working distance of the objective lens is also important: sufficient spacing between the cryosample and the ambient temperature objective lens is required to ensure that the sample is not inadvertently heated by accidental contact or limited convective cooling.

Finally, the magnification of the objective lens is also an important parameter. While the magnification should be high enough to reach the Nyquist limit for the pixel size, excessive magnification can decrease the signal to noise ratio. With the high quantum efficiency and low readout and dark noise of the latest generation sCMOS detectors, in combination with the long lifetime of single-molecule events in cryogenic conditions, commonly available magnifications of 63× and 100× both meet the requirements.

In this microscope, we use only a single objective lens with a working distance of 2 mm, an NA of 0.9, a 100× magnification, and approximately a 130 µm wide field of view. Although the addition of a second, lower magnification lens could facilitate finding areas of interest within a sample, we opt for the use of a single lens to avoid contamination of the sample that would occur during repeated switching of the lenses (see below).

Sample stage

The defining characteristic of a fluorescence cryo-microscope is the sample stage, which should at all times maintain the sample at low enough temperature while also providing access to an objective lens. A number of custom-built stages have been described[24-26], but the significant investment and effort required to procure or design such stages make commercially available stages a more practical option for a group interested in using SR-cryoCLEM rather than developing it. At the time of writing, the CMS196 cryostage design by Linkam Scientific Instruments Ltd. is widely used, but there are some alternatives such as a stage by Leica that is part of a larger widefield cryo-fluorescence microscopy system.

Our design employs the Linkam CMS196v3. This is a low-profile stage that is relatively easy to integrate into a custom microscope, but also suffers from certain disadvantages – including contamination of the sample due to exposure to air, high drift, and short cold times – yet, these problems can all be mitigated by the use of flow cabinets, post-acquisition drift correction, and automated liquid nitrogen refilling devices.

We do not currently make use of a flow cabinet, with which the stage or the entire microscope could be maintained in a low humidity environment (see for example[27]). However, a simple sleeve wrapped around the objective lens that seals the gap between the lens and the top of the stage through which humid air could flow in reduces the contamination rate. In the future, better sample stages – ideally ones that interface with cryoEM sample transport systems – might become available that are less prone to drift, require less frequent refilling, and better seal the sample compartment in order to avoid ice contamination.

Parts list

In this section we provide an overview of the parts used in the cryoscope and discuss several alternatives. While it is possible to build a copy of our microscope with the exact parts listed below, we would recommend that prospective users investigate alternative components that are either i) better suited for their particular application; e.g., for a single-color SMLM setup, a laser engine with a single source in combination with a spontaneously blinking fluorescent protein could be sufficient, in which case the cost can be reduced by ~25k, or ii) improved components brought to market after publication of this chapter, such as alternative cryostages.

[TABLE 1 GOES HERE]

The most expensive component is the laser light engine – commercial devices typically cost tens of thousands of euros. The steep prices of certain components are well known

and, although in some cases warranted (e.g. filters and detectors), in other cases large expenditures can be avoided by building custom hardware. This is particularly the case for acquisition control devices and laser light sources. As such, a number of popular open-source laser source [28,29] and controller[30,31] alternatives have been developed. Whereas we make use of a commercial laser source, labs that have the required expertise and time may opt for a custom solution. For acquisition control we make use of a 'triggerbox'; an Arduino connected to the camera, light sources, and PC, which efficiently synchronizes all of the imaging hardware after it receives a user's instructions via the microscope control software.

Software

A number of options are available for microscope control software. Two examples are µManager, a versatile program that is widely used for diverse imaging applications[32,33] and PYME, an open-source Python package designed specifically for SMLM[34]. During development of our cryoscope, we found that our software requirements were best met with custom software (Figure 2), which is available on our GitHub repository (github.com/bionanopatterning/cryoscope_2). Unlike e.g. PYME, this software was not written for general use, but with the limited scope of controlling our particular hardware and triggering setup. We therefore generally recommend PYME, but refer those interested in a similar custom approach to our software.

[FIGURE 2 GOES HERE]

Construction

The design of the cryoscope is largely modular and simple, in the sense that the number of components is low and assembly is straightforward. The triggerbox, mentioned above, provides an interface to connect the light sources, camera, and the PC (Figure 3a). We use a breadboard mounted on solid steel posts on a vibration-reducing optical table as a construction platform (label b in Figure 3). The laser illumination, LED illumination, and imaging arms of the optical path (labels C, D, E, respectively) can be assembled in isolation and are subsequently attached to the construction platform via a simple connecting interface. The focusing and filter stage (F) is a single off-the-shelf component. Finally, the cryostage is mounted in a holder that allows for careful alignment of the stage position, which in turn is carried by a manual vertical positioning stage with which the stage can be engaged to the microscope.

[FIGURE 3 GOES HERE]

A number of parts require custom machining: 1) the focus and filter stage is not originally intended for mounting to a breadboard, and was modified for us by the supplier, 2) a hole must be cut in the breadboard, as the imaging path runs through it – this modification can also be requested from the supplier, 3) the tube lens is not designed for mounting to a breadboard and a custom adapter is required for this purpose, and 4) a custom dovetail is required to connect the cryostage mount to the vertical translation platform. These

latter two parts are simple enough to fabricate that either a supplier or a local workshop should be able to create it.

Finally, we use a 3D-printed housing for the triggerbox and to hold the beam splitter that combines the laser and LED illumination paths. Since the LED source is used for reflection imaging, which does not require bright illumination, a thin, low-reflectivity mirror is optimal for combining the laser and LED sources: it transmits most of the laser light, but also reflects a low fraction of the LED source. In our experience, a simple glass cover slip is ideally suited for this purpose.

The figures below provide detailed views and additional information on each of the modules used in the construction of the cryoscope. 3D models of the full design can be downloaded at ccb.lumc.nl/downloads-231.

Mounting

[FIGURE 4 GOES HERE]

Laser illumination path

[FIGURE 5 GOES HERE]

Imaging path

[FIGURE 6 GOES HERE]

Cryostage

[FIGURE 7 GOES HERE]

LED illumination path

[FIGURE 8 GOES HERE]

Results

Here we showcase an experiment that is representative of the correlated SMLM and cryoEM workflow. We used our microscope to perform SMLM on U2OS cells expressing rsEGFP2-Vimentin grown on 1.2/1.3 holey gold UltrAuFoil grids (Figure 9), but the data acquisition procedure and fluorescent label that we use (rsEGFP2) are generally applicable to any sample.

In our experience, a single-molecule localization map suited for use in identifying regions of interest for cryoEM acquisition can be acquired in only ~5 minutes once an appropriate region of the sample is found. Finding a region of interest typically also requires a few minutes.

To create a single-molecule localization map that is suited for localizing structures of interest for subsequent cryoEM inspection, we typically use a total fluorescence imaging time of 100 seconds, e.g., 500 frames with 200 ms exposure time (Figure 9a), and an illumination power density on the order of 100–200 W/cm^2, depending on the grid type[35].

This is a relatively low number of frames, but it is sufficient to generate a useful SMLM image (Figure 9b, c), and since there are usually many sites of interest in one sample we currently prefer to image a larger number of sites briefly rather than extensively image a few.

Next to the fluorescence images we also expose the sample to 405 nm light in order to activate rsEGFP2 (Figure 9d) and we acquire reflection images using 528 nm LED illumination and the same filter cube as used for fluorescence imaging, which partially transmits 528 nm light (Figure 9e). These reflected light images are very useful for correlation of light to electron microscopy images.

Even though deactivation of fluorescent proteins is significantly impaired at 76 K in comparison to ambient temperature, many single-molecule events can be observed (Figure 9f-g) – particularly in thin or sparsely labelled regions of the sample: the image in Figure 9b comprises 900.000 individual localizations.

[FIGURE 9 GOES HERE]

Multiple cells or regions of interest can be imaged on a single grid within a relatively short timespan; a well-trained operator can perform a SMLM imaging experiment on 5-10 sites of interest within one to two hours, including retrieving samples from storage, cooling down the sample stage, and returning samples to storage after the imaging is completed. Screening multiple grids is also facile: a grid box can be kept in the cryostage during imaging, and swapping grids from the gridbox onto the stage takes only about a minute.

Finally, SMLM imaging of cryosamples is highly compatible with cryoEM imaging. Provided illumination power densities are kept in check, samples are not devitrified by fluorescence imaging, and prolonged high-power laser illumination has also been found not to affect achievable resolution in single-particle analysis protein structure determination[36]. We believe that the combination of cryoEM and cryoSMLM is a very promising method: it allows for the localization of specifically labelled proteins of interest within the context of high-resolution electron microscopy images, thus enriching cryoEM data and enabling accurately targeted cryoEM data acquisition, which could vastly increase throughput of cryoEM imaging of rare, transient or hard to identify structures.

Conclusions

In the above, we've outlined the design of a microscope suited for cryo-single molecule localization imaging and demonstrated its use by imaging rsEGFP2-Vimentin expressing U2OS that were grown on grids for cryoEM imaging. One acquisition, which requires only ~5 minutes of imaging time, can result in hundreds of thousands of single-molecule localizations across an area of ~100 μm^2. Within this area, one can typically identify numerous sites of interest that are also suited for cryo-electron tomography imaging. The combination of super-resolution fluorescence microscopy and cryoEM is thus a feasible and, in our experience, even a routine method that can be to accurately locate

sites of interest for cryoEM and enrich cryoEM data with the context provided by single-molecule localization maps.

Future developments in hardware (e.g. new cryostages and cryo-sample transfer systems), software (e.g. for correlation), and methodology (e.g. novel fluorophores with enhanced switching characteristics) will help improve localization accuracy, sample cleanliness, imaging throughput, and many other aspects of correlated cryo-microscopy, and we are optimistic that the advantages offered by the combination of these two high-resolution imaging methods will be recognized by and accessible to increasingly more researchers. To this we hope that our design can make a contribution, and we are therefore open to communications about adaption and further development of our and similar microscope designs.

References

1 Dahlberg, P. D. *et al.* Cryogenic single-molecule fluorescence annotations for electron tomography reveal in situ organization of key proteins in Caulobacter. *Proceedings of the National Academy of Sciences* **117**, 13937-13944 (2020). https://doi.org:10.1073/pnas.2001849117

2 Dahlberg, P. D. & Moerner, W. E. Cryogenic Super-Resolution Fluorescence and Electron Microscopy Correlated at the Nanoscale. *Annu Rev Phys Chem* **72**, 253-278 (2021). https://doi.org:10.1146/annurev-physchem-090319-051546

3 Tuijtel, M. W., Koster, A. J., Jakobs, S., Faas, F. G. A. & Sharp, T. H. Correlative cryo super-resolution light and electron microscopy on mammalian cells using fluorescent proteins. *Scientific Reports* **9**, 1369 (2019). https://doi.org:10.1038/s41598-018-37728-8

4 Last, M. G. F., Voortman, L. M. & Sharp, T. H. Measuring cryo-TEM sample thickness using reflected light microscopy and machine learning. *J Struct Biol* **215**, 107965 (2023). https://doi.org:10.1016/j.jsb.2023.107965

5 Au - Vyas, N. *et al.* Cryo-Structured Illumination Microscopic Data Collection from Cryogenically Preserved Cells. *JoVE*, e62274 (2021). https://doi.org:doi:10.3791/62274

6 Moser, F. *et al.* Cryo-SOFI enabling low-dose super-resolution correlative light and electron cryo-microscopy. *Proc Natl Acad Sci U S A* **116**, 4804-4809 (2019). https://doi.org:10.1073/pnas.1810690116

7 Kaufmann, R. *et al.* Super-resolution microscopy using standard fluorescent proteins in intact cells under cryo-conditions. *Nano Lett* **14**, 4171-4175 (2014). https://doi.org:10.1021/nl501870p

8 Schermelleh, L. *et al.* Super-resolution microscopy demystified. *Nature Cell Biology* **21**, 72-84 (2019). https://doi.org:10.1038/s41556-018-0251-8

9 Lelek, M. *et al.* Single-molecule localization microscopy. *Nature Reviews Methods Primers* **1**, 39 (2021). https://doi.org:10.1038/s43586-021-00038-x

10 Betzig, E. *et al.* Imaging Intracellular Fluorescent Proteins at Nanometer Resolution. *Science* **313**, 1642-1645 (2006). https://doi.org:10.1126/science.1127344

11 Rust, M. J., Bates, M. & Zhuang, X. Sub-diffraction-limit imaging by stochastic optical reconstruction microscopy (STORM). *Nature Methods* **3**, 793-796 (2006). https://doi.org:10.1038/nmeth929

12 Hohlbein, J. *et al.* Open microscopy in the life sciences: quo vadis? *Nature Methods* **19**, 1020-1025 (2022). https://doi.org:10.1038/s41592-022-01602-3

13 Danial, J. S. H. *et al.* Constructing a cost-efficient, high-throughput and high-quality single-molecule localization microscope for super-resolution imaging. *Nature Protocols* **17**, 2570-2619 (2022). https://doi.org:10.1038/s41596-022-00730-6

14 Holm, T. *et al.* A Blueprint for Cost-Efficient Localization Microscopy. *ChemPhysChem* **15**, 651-654 (2014). https://doi.org:10.1002/cphc.201300739
15 Kaufmann, R., Hagen, C. & Grünewald, K. Fluorescence cryo-microscopy: current challenges and prospects. *Current Opinion in Chemical Biology* **20**, 86-91 (2014). https://doi.org:10.1016/j.cbpa.2014.05.007
16 Faro, A. R. *et al.* Low-temperature switching by photoinduced protonation in photochromic fluorescent proteins. *Photochemical & Photobiological Sciences* **9**, 254-262 (2010). https://doi.org:10.1039/b9pp00121b
17 Schwartz, C. L., Sarbash, V. I., Ataullakhanov, F. I., McIntosh, J. R. & Nicastro, D. Cryo-fluorescence microscopy facilitates correlations between light and cryo-electron microscopy and reduces the rate of photobleaching. *Journal of Microscopy* **227**, 98-109 (2007). https://doi.org:10.1111/j.1365-2818.2007.01794.x
18 Phillips, M. A. *et al.* CryoSIM: super-resolution 3D structured illumination cryogenic fluorescence microscopy for correlated ultrastructural imaging. *Optica* **7**, 802-812 (2020). https://doi.org:10.1364/OPTICA.393203
19 Bourgeois, D. & Adam, V. Reversible photoswitching in fluorescent proteins: A mechanistic view. *IUBMB Life* **64**, 482-491 (2012). https://doi.org:10.1002/iub.1023
20 Dahlberg, P. D., Perez, D., Hecksel, C. W., Chiu, W. & Moerner, W. E. Metallic support films reduce optical heating in cryogenic correlative light and electron tomography. *Journal of Structural Biology* **214**, 107901 (2022).
21 Last, M. G. F., Tuijtel, M. W., Voortman, L. M. & Sharp, T. H. Selecting optimal support grids for super-resolution cryogenic correlated light and electron microscopy. *Scientific Reports* **13** (2023). https://doi.org:10.1038/s41598-023-35590-x
22 Le Gros, M. A., McDermott, G., Uchida, M., Knoechel, C. G. & Larabell, C. A. High-aperture cryogenic light microscopy. *Journal of Microscopy* **235**, 1-8 (2009). https://doi.org:10.1111/j.1365-2818.2009.03184.x
23 Wang, L. *et al.* Solid immersion microscopy images cells under cryogenic conditions with 12 nm resolution. *Communications Biology* **2**, 74 (2019). https://doi.org:10.1038/s42003-019-0317-6
24 Xu, X. *et al.* Ultra-stable super-resolution fluorescence cryo-microscopy for correlative light and electron cryo-microscopy. *Science China Life Sciences* **61**, 1312-1319 (2018).
25 Nahmani, M., Lanahan, C., DeRosier, D. & Turrigiano, G. G. High-numerical-aperture cryogenic light microscopy for increased precision of superresolution reconstructions. *Proceedings of the National Academy of Sciences* **114**, 3832-3836 (2017). https://doi.org:10.1073/pnas.1618206114
26 Sartori, A. *et al.* Correlative microscopy: Bridging the gap between fluorescence light microscopy and cryo-electron tomography. *Journal of Structural Biology* **160**, 135-145 (2007). https://doi.org:https://doi.org/10.1016/j.jsb.2007.07.011
27 Tacke, S. *et al.* A streamlined workflow for automated cryo focused ion beam milling. *Journal of Structural Biology* **213**, 107743 (2021). https://doi.org:10.1016/j.jsb.2021.107743
28 Nicovich, P. R., Walsh, J., Böcking, T. & Gaus, K. NicoLase—An open-source diode laser combiner, fiber launch, and sequencing controller for fluorescence microscopy. *PLOS ONE* **12**, e0173879 (2017). https://doi.org:10.1371/journal.pone.0173879
29 Schröder, D., Deschamps, J., Dasgupta, A., Matti, U. & Ries, J. Cost-efficient open source laser engine for microscopy. *Biomed. Opt. Express* **11**, 609-623 (2020). https://doi.org:10.1364/BOE.380815
30 Martens, K. J. A. *et al.* Visualisation of dCas9 target search in vivo using an open-microscopy framework. *Nature Communications* **10**, 3552 (2019). https://doi.org:10.1038/s41467-019-11514-0

31 Colville, M. J., Park, S., Zipfel, W. R. & Paszek, M. J. High-speed device synchronization in optical microscopy with an open-source hardware control platform. *Scientific Reports* **9**, 12188 (2019). https://doi.org:10.1038/s41598-019-48455-z

32 Edelstein, A., Amodaj, N., Hoover, K., Vale, R. & Stuurman, N. Computer control of microscopes using μManager. *Curr Protoc Mol Biol* **Chapter 14**, Unit14.20 (2010). https://doi.org:10.1002/0471142727.mb1420s92

33 Edelstein, A. D. *et al.* Advanced methods of microscope control using μManager software. *J Biol Methods* **1** (2014). https://doi.org:10.14440/jbm.2014.36

34 Susano Pinto, D. M. *et al.* Python-Microscope – a new open-source Python library for the control of microscopes. *Journal of Cell Science* **134**, jcs258955 (2021). https://doi.org:10.1242/jcs.258955

35 Last, M. G. F., Tuijtel, M. W., Voortman, L. M. & Sharp, T. H. Selecting optimal support grids for super-resolution cryogenic correlated light and electron microscopy. *bioRxiv* (2022). https://doi.org:10.1101/2022.12.05.519127

36 Last, M. G. F., Noteborn, W. E. M., Voortman, L. M. & Sharp, T. H. Super-resolution fluorescence imaging of cryosamples does not limit achievable resolution in cryoEM. *bioRxiv*, 2023.2003.2008.531682 (2023). https://doi.org:10.1101/2023.03.08.531682

[TABLE 1 BELOW]

Description	***Supplier***	***Item ID***	***Cost (€)***	**ID**
Laser illumination module			~50600	
Laser light engine w. SM fiber with sources: 405 nm / 100 mW 488 nm / 120 mW 561 nm / 150 mW	Omicron-Laserage	LightHUB	50000	1
XY adjustable fiber mount + fiber adapter	Thorlabs	CXY1	200	2
Lens mounts	Thorlabs	CP33M	17 x 2	3
Assembly mount	Thorlabs	CP36M	22	4
Adjustable diaphragm field stop	Thorlabs	CP20D	102	5
Cage rods	Thorlabs	ER12	17 x 4	6
Collection lens	Thorlabs	LBF254-075	50	7
Field lens	Thorlabs	LA4874-A	100	8
Cage system attachment plate	ASI	C60-30CRM-30LM	100	9
LED illumination module			~15600	
LED light source w. LLG with sources: 405 nm, 470 nm, 532 nm	Omicron-Laserage	LedHUB	15000	10
Various mounts	Thorlabs	AP90RLM	191	11
	Thorlabs	CF175C	14	12
	Thorlabs	PH50E	28	13
	Thorlabs	TR50	6	14
	Thorlabs	CP33M	17	3
	Thorlabs	AD11F	33	15
Beam combining mirror		24 x 32 mm cover slip	0	16
Beam combiner mount	Custom made		0	17
Reflection imaging beamsplitter	Thorlabs	BSW26R	306	
Imaging			~35000	
Tube lens	ASI	C60-TUBE-B	1000	18
C-Mount adapter	ASI	C60-3060-C-MOUNT	225	19

Tube lens to breadboard adapter	Custom made		150	20
Focus and filter stage	ASI	MIM4 Slider Nikon	6000	21
Focus and filter stage controller	ASI	MS1+1	4000	
Camera	pco	edge 4.2 bi wc	17000	22
Objective lens	Nikon	TU Plan Apo 100/0.9	6500	23
Sample stage			~22200	
Cryostage	Linkam Scientific	CMS196v3	20000	24
Vertical translation manual stage	Thorlabs	VAP4_M	800	
Cryostage mount	Zeiss		1300	
Cryostage mount adapter	Custom made		100	
Filters			~2000	
BFP channel – emission	Thorlabs	MF460-60	255	
BFP channel - dichroic	Thorlabs	MD416	277	
GFP channel – emission	Semrock	FF01-525/50	350	
GFP channel – dichroic	Semrock	FF495-Di03	390	
RFP channel – emission	Semrock	FF01-630/92	400	
RFP channel – dichroic	Semrock	FF570-Di01	280	
Mounting			~3500	
Optical table – frame	Thorlabs	SDP6090	1828	30
Optical table – breadboard	Thorlabs	B6090	1259	31
Microscope breadboard	Thorlabs	MB3045	195	25
Microscope breadboard support	Thorlabs	P300M	96 x 4	26
Acquisition control			~2300	
PC + accessories			2000	
Arduino Leonardo			30	27
Arduino Housing	Custom made		0	28
Cables and connectors	Dependent on camera and light sources		10 x 25	29
Approximate total cost			**€131000**	

Table 1 – list of parts used in the construction of the cryoscope. The list is subdivided into modules (blue headers), some of which (e.g. the LED illumination module) are not absolutely required for SMLM. Suppliers and supplier item IDs are indicated, as well as the approximate cost (€) of the part. This approximation is the most inaccurate for the more expensive parts: light sources, cameras, filters, and objective lenses vary in price depending on the chosen supplier and specifications. Shipping and customs fees, which can be significant, are not included. The rightmost column, 'ID', lists the labels used in Figure 4.

Figures

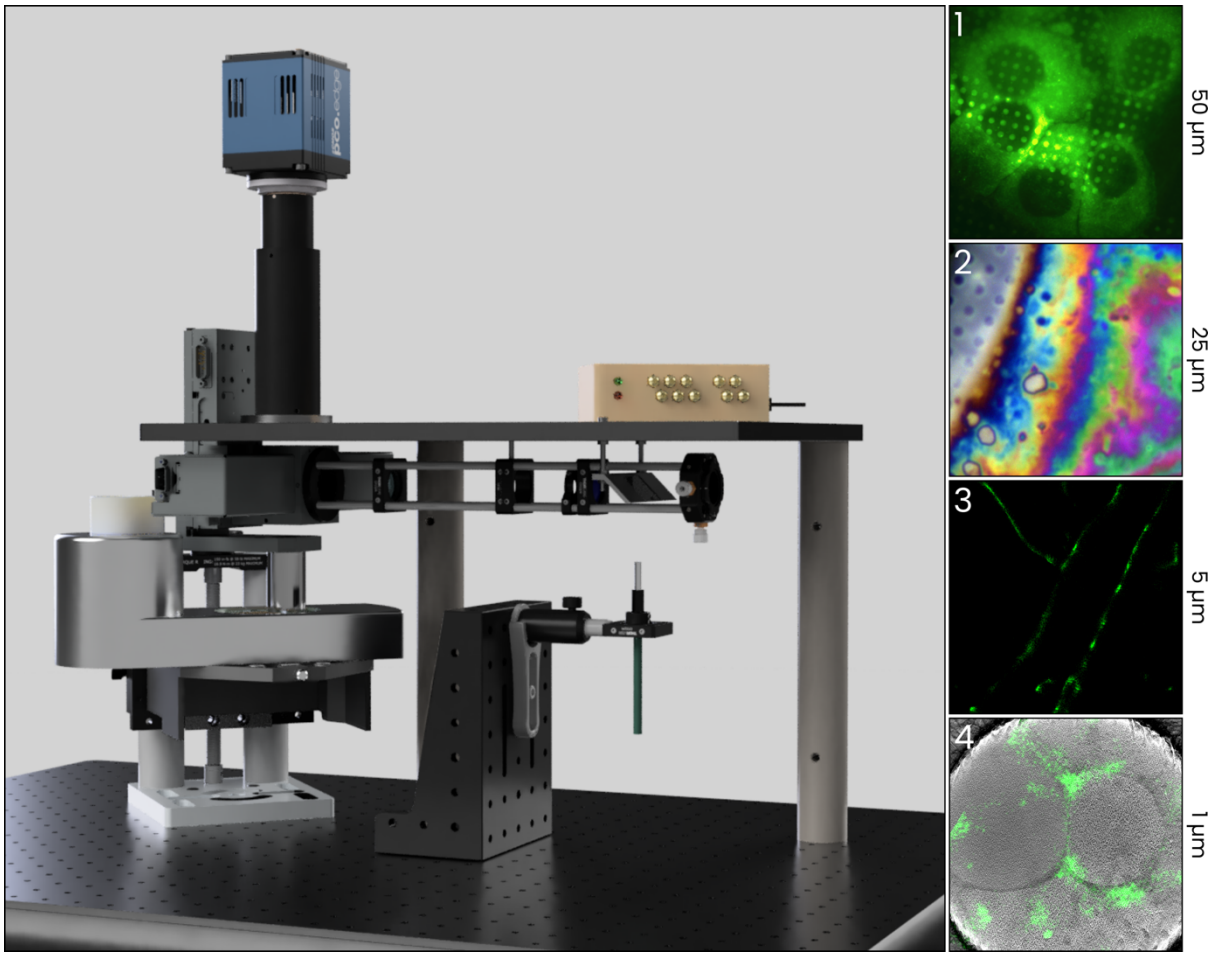

Figure 1 – Design of the cryoscope and some exemplary results. The main image shows a 3D model of the cryoscope – as can be seen, the optical system is relatively simple and modular. In the adjacent panels, images at various scales acquired with the cryoscope are displayed: 1) U2OS cells expressing rsEGFP2-IMPDH2 grown on a holey gold TEM grid (50 µm field of view), 2) an example of a three-color composite reflected light image of a cell, which can be used to determine the sample thickness (25 µm), 3) a super-resolution image of rsEGFP2-Vimentin (5 µm) in a U2OS cell, and 4) a single molecule localization map of rsEGFP2-TAP1, a membrane protein of the endoplasmic reticulum, correlated with cryo-electron tomgraphy data that reveals colocalization of fluorescent signal and vesicles.

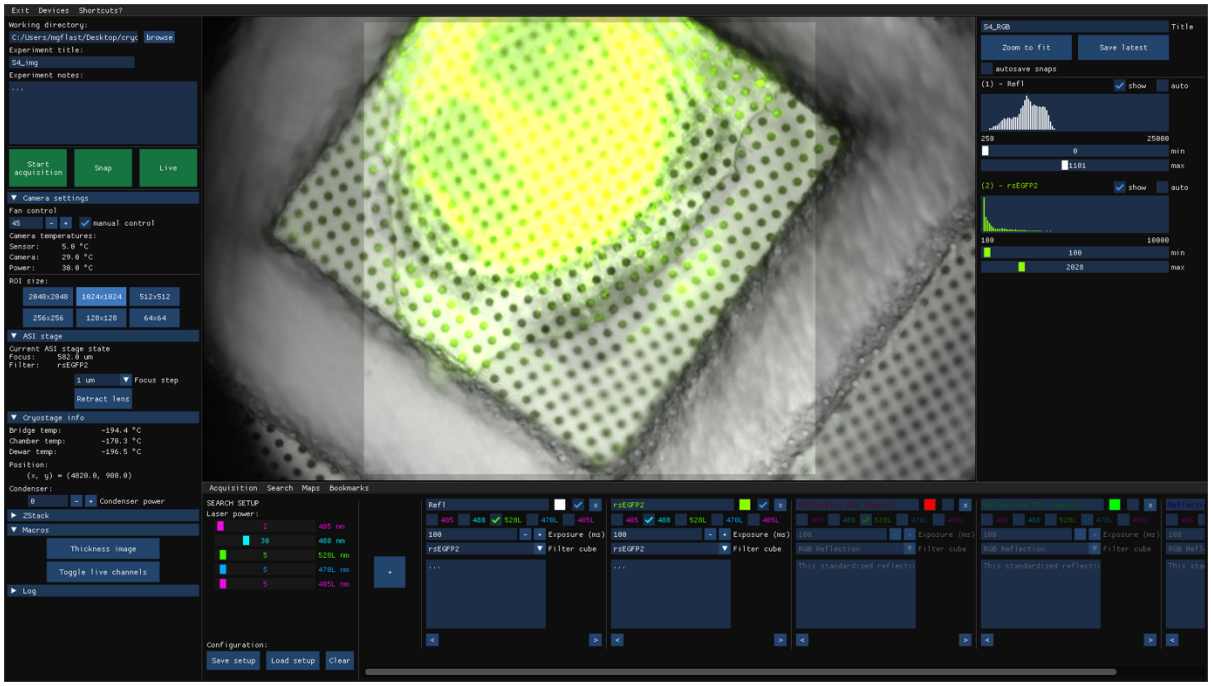

Figure 2 – a view of the cryoscope acquisition software. In the left column, the status and configuration of the cryostage, camera, and focus and filter stage, can be inspected and controlled, and a number of other settings are available. In the horizontal bottom menu, acquisition sequences can be set up, in a minimal yet versatile interface. The column on the right allows for adjusting contrast of live images. The image in the centre is a composite image showing rsEGFP2-TAP1 fluorescence (green) in an U2OS cell grown on a holey gold support film, which is highly reflective (gray)

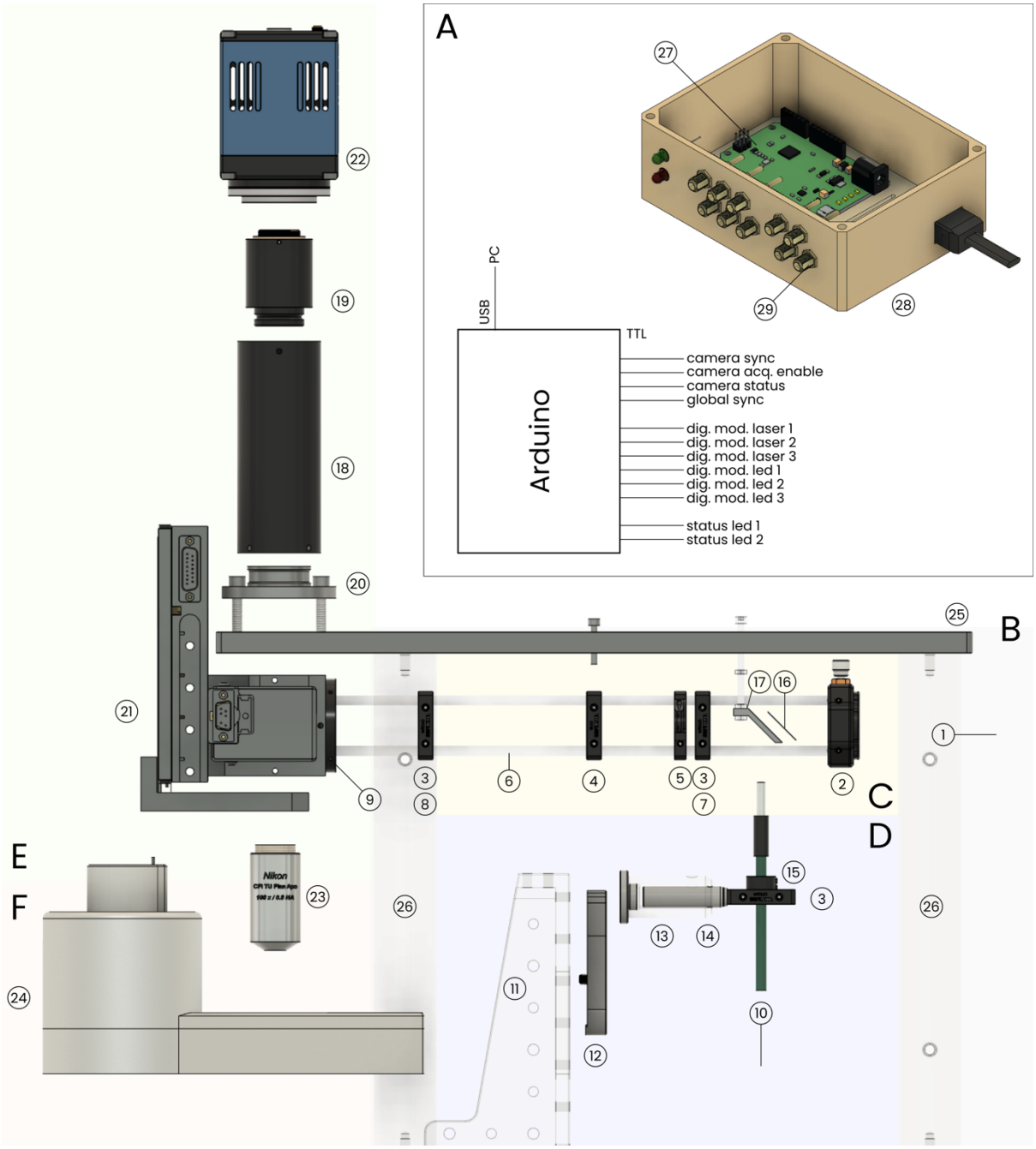

Figure 3 – annotated exploded view of the cryoscope. Number tags indicate items listed in Table 1. Background colors as well as labels indicate modules: the triggerbox (A, white), construction platform (B, gray), excitation light path (C, yellow), LED illumination path (D, blue), imaging path (E, green), and the cryostage (F, red).

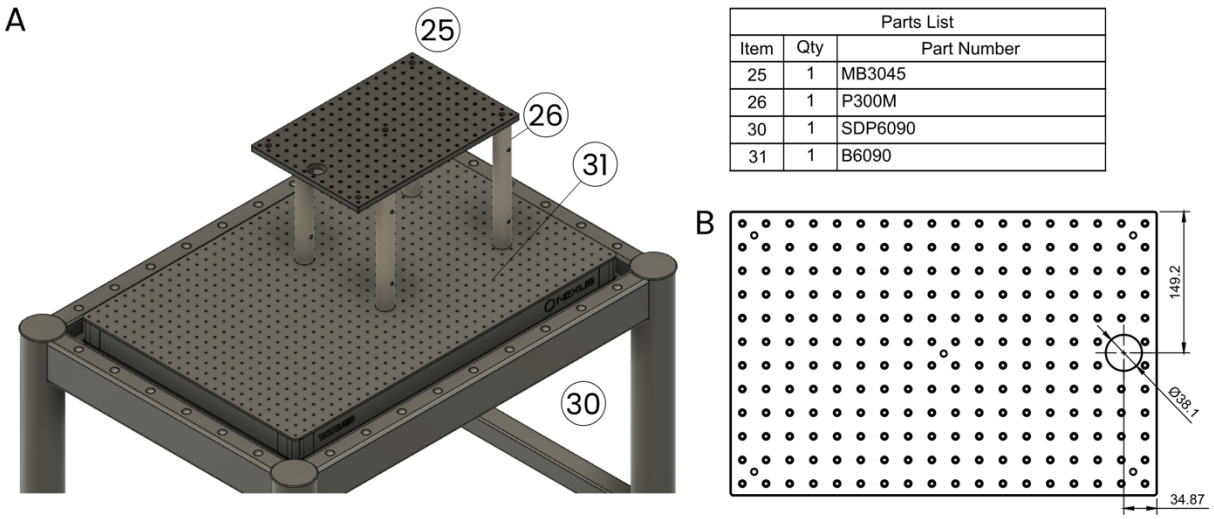

Parts List		
Item	Qty	Part Number
25	1	MB3045
26	1	P300M
30	1	SDP6090
31	1	B6090

Figure 4 – A view of the mounting platform onto which the cryoscope is assembled. A) 3D view of the mounting platform assembled on the optical table. Parts are tagged by numbers and listed in the adjacent table. B) A drawing specifying the required modifications to the breadboard.

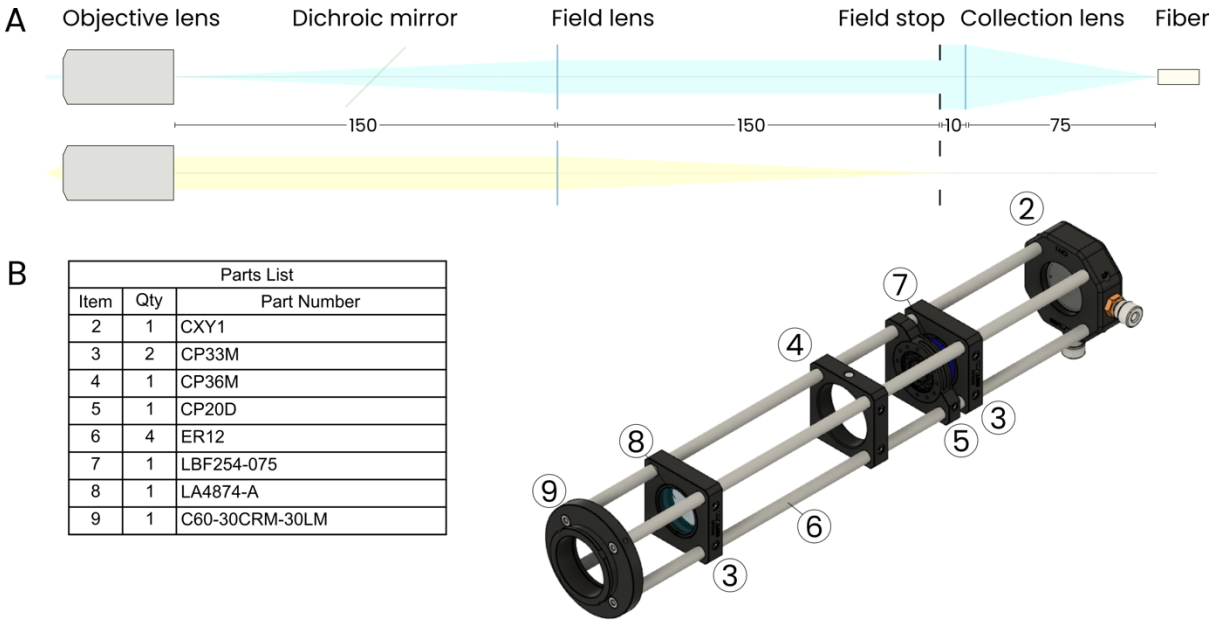

Parts List		
Item	Qty	Part Number
2	1	CXY1
3	2	CP33M
4	1	CP36M
5	1	CP20D
6	4	ER12
7	1	LBF254-075
8	1	LA4874-A
9	1	C60-30CRM-30LM

Figure 5 – The laser illumination path. A) Two schematics representing the path traversed by laser light (top), and the positioning of the field lens and field stop (bottom). B) 3D model of the laser illumination path, with number tags corresponding to items listed in the adjacent table.

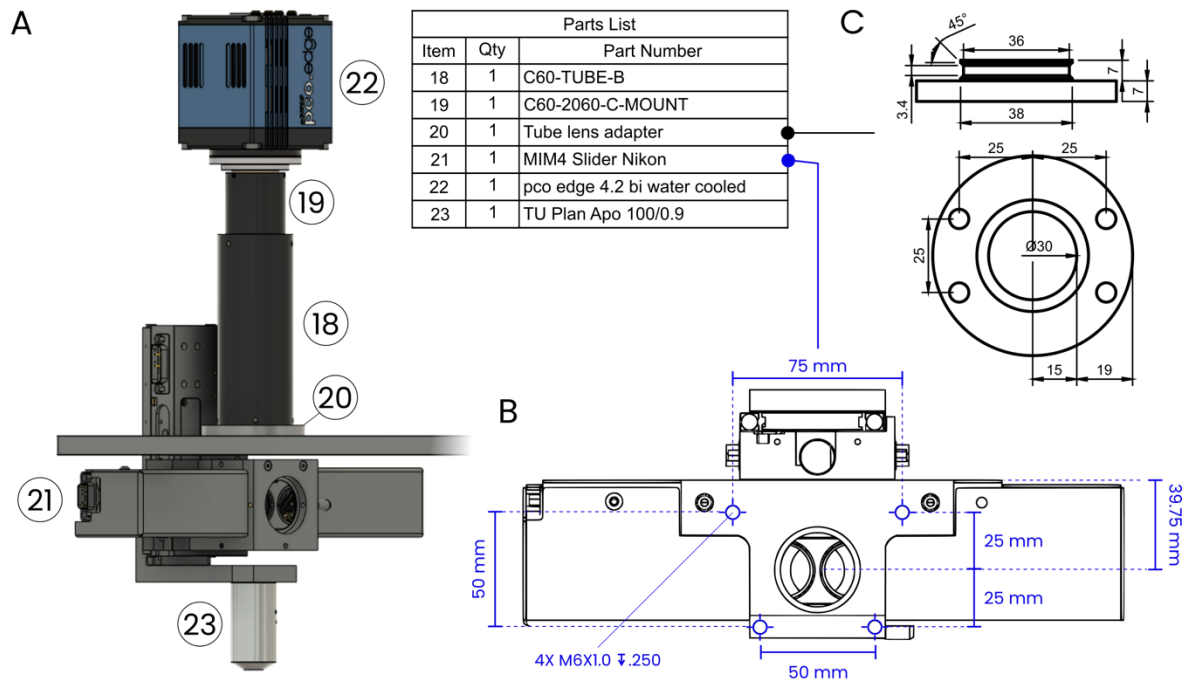

Figure 6 – The imaging path. A) A view of the imaging path, comprising the camera, objective lens, and the combined focus and filter cube stage. Items corresponding to the indicated numbers are listed in the adjacent table. B) A drawing specifying the required modifications to the filter and focus stage. Four M6 threaded holes are drilled in the top to allow for mounting to the underside of the assembly breadboard. The supplier (Applied Scientific Instrumentation) modified this part for us; refer to the C60-SLIDER-LUMC modification. C) A drawing specifying the design of the custom adapter that we use to mount the tube lens to the assembly breadboard.

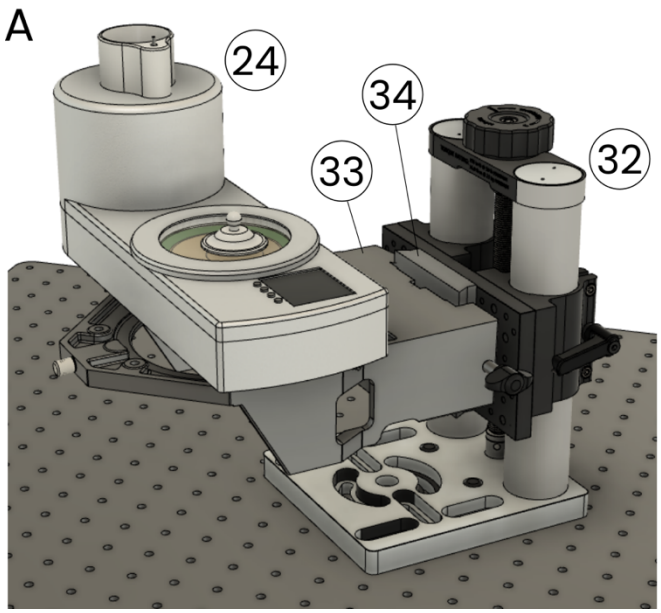

		Parts List
Item	Qty	Part Number
24	1	CMS196v3
32	1	VAP4M
33	1	430704-9901
34	1	Zeiss dovetail adapter

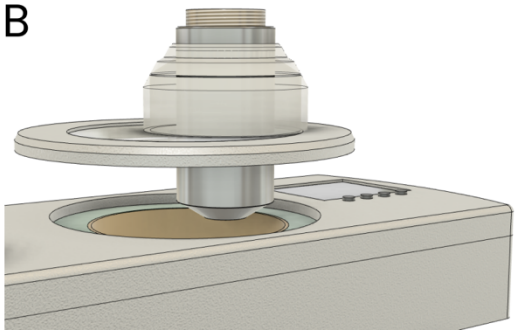

Figure 7 – The positioning of the cryostage. A) A view of the cryostage mounted on the cryostage holder (Zeiss), which is in turn mounted onto a manual vertical positioning stage that is used to engage the stage to the microscope. B) A close-up of the cryostage with the objective lens and a protective sleeve inserted through the lid of the stage. During operation the lid covers the sample chamber – in the image here, the lid is offset vertically for illustrative purpose.

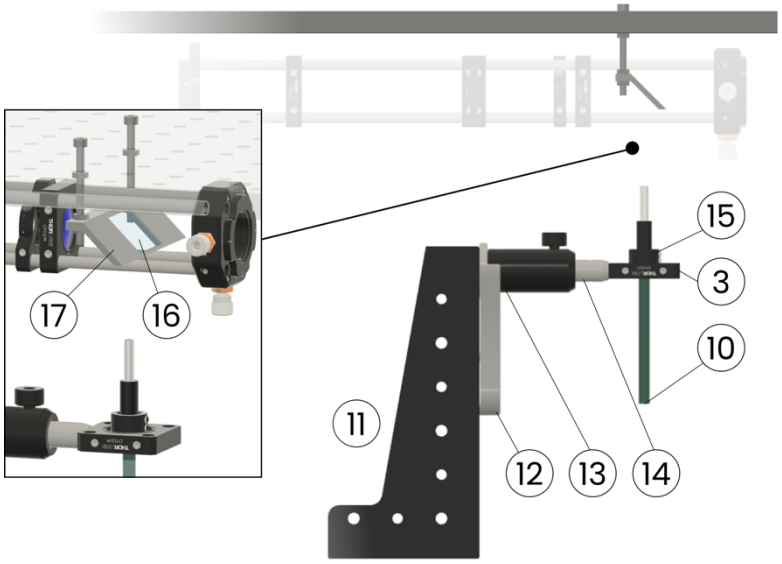

		Parts List
Item	Qty	Part Number
3	1	CP33M
10	1	LedHUB
11	1	AP90RLM
12	1	CF175C
13	1	PH50E
14	1	TR50
15	1	AD11F
16	1	24 x 32 mm cover slip
17	1	Beam combiner mount

Figure 8 – Detailed view of the LED illumination module. After constructing the cryoscope without the LED illumination module, this module can be retrofitted into the microscope. The base (parts 3, 10-15) is simply placed on the optical table and the beam combining mirror is mounted in a 3D printed holder that can be inserted into the laser illumination path (see inset). Part names are listed in the adjacent table.

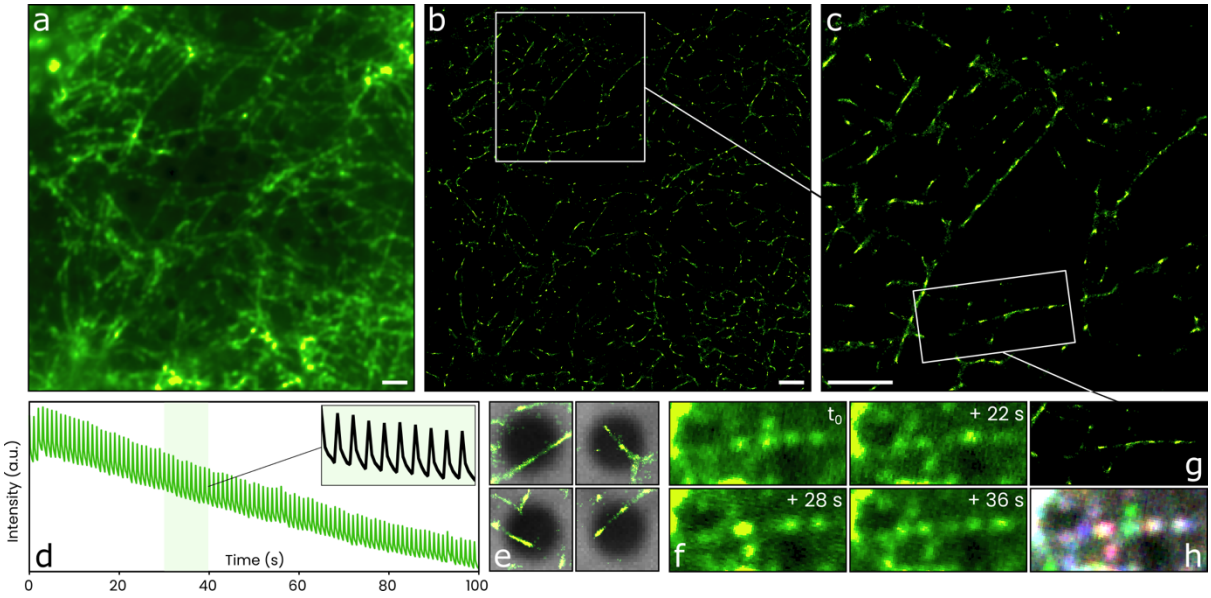

Figure 9 – cryo-SMLM imaging of Vimentin, labelled with rsEGFP2, in a U2OS cell. a) Sum projection image of a 500 frame timelapse video of rsEGFP2 fluorescence. To activate the fluorescent protein, a brief 405 nm illumination pulse was applied after every 5 fluorescence frames. b) Single-molecule localization map (900,000 localizations) generated using the same dataset. c) Magnified section of the region indicated by the white square in panel b. d) A plot of mean fluorescence intensity per frame versus time since the start of the acquisition. After every 405 nm pulse, the overall fluorescence intensity of the frames increases as many molecules of rsEGFP2 are activated, and then decreases again as fluorescence is excited by 488 nm illumination, which also deactivates rsEGFP2. The inset shows a section of the graph magnified. e) Examples of regions that could be interesting for cryoEM data acquisition. Vimetin filaments can be recognized in the localization map (green), which is overlayed on reflected light images (gray) that show holes (1.2 µm) in the holey gold sample support film. f) Single frames from the timelapse dataset, showing the same region of the sample at different moments in time. Where a filament is seen in the final reconstruction (see panel g), fluorescence from individual molecules can be seen in the frames. g) The region of the single-molecule localization map corresponding to the frames shown in panel f. h) Three of the images in panel f combined into a composite RGB image, to visualize the relative location of the single molecule fluorescence spots. Scale bars are 2 µm.